

A SPIRALED SEGMENTED WAVEGUIDE SENSOR: PRINCIPLE AND EXPERIMENT

Joris van Lith, Paul.V. Lambeck, Hugo.J.W.M. Hoekstra, Rene. G. Heideman, R.R. Wijn,
IOMS, MESA⁺-institute, University of Twente, P.O. Box 217,
7500 AE Enschede, the Netherlands
P.V.Lambeck@el.utwente.nl

SUMMARY

A novel type of chemo-optical sensor has been designed, fabricated and characterized. The sensor is simple to fabricate, puts low demands on light source quality and shows resolution of index changes of $\sim 3 \cdot 10^{-8}$

KEYWORD

Segmented waveguides, sensing, guided-wave optics, integrated optics

ABSTRACT

INTRODUCTION

Integrated optical (IO) sensor systems have a large potential to be small, very sensitive and relatively cheap [1]. A novel type of IO sensor based on a segmented waveguide, in which chemically induced changes of refractive index are read out as index dependent losses, has been investigated. Segmented waveguides have raised a lot of interest due to their potential as devices for quasi-phase matching in second harmonic generation [1] or for tuning the size of the modal field [2,3], but up until recently [5-8] they never have been used for sensing purposes.

The segmented waveguide (SW) sensor has low demands on the technology and on the quality of the light source, but still enables high resolution. The sensor can be used as an on/off alarm sensor or for continuous measurements. Using standard peripheral equipment a resolution of $\delta n = 3 \cdot 10^{-8}$ is expected to be feasible. In the rest of this paper first the device principle will be explained, next theoretical and design aspects will be discussed. This is followed by the presentation of experimental results of measurements on a few realised devices, and a section with conclusions.

DEVICE PRINCIPLE

An SWS is a waveguide channel which consists of at least two types of segments. In case of a monomodal waveguide, at each transition between two adjacent segments power is coupled from the guided mode of one

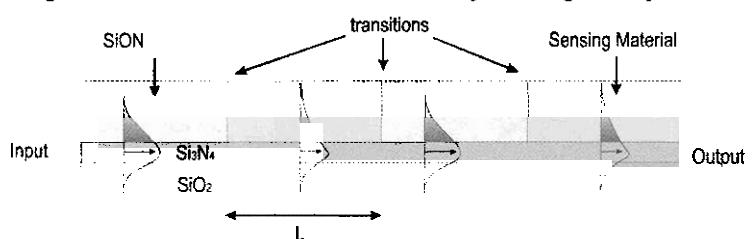


Figure 1. Longitudinal cross-section of the sensor (4 segments).

segment into the guided mode of the next segment. The coupling efficiency is determined mainly by the degree of similarity of the mode profiles in both types of segments. The shape of the mode profile in the so called 'active' segments depends on the refractive index of the sensing material that has been incorporated in the segment. In

the other type of segments this dependency is different or even absent. This dependency is different for both types of segments. This way the coupling efficiency is a function of the refractive index of the sensing material. The segmentation in the waveguide channel can be realized in various ways. The two types of segments may differ with respect to the cladding material, but also with respect to the core material, or the width of the waveguide channel. In this section the principle will be explained in more detail for a specific type of segmentation: segmentation of the cladding.

In figure 1 a longitudinal cross-section of the sensing part is depicted: a ridge type wave-guiding channel consisting alternately of two types of segments: segments with SiON as cladding and segments with a sensing material as cladding. The sensing material is a chemically active material whose refractive index depends on the concentration, c , of a specific chemical compound. A guided mode is launched into the first segment of the waveguide. We define the difference in refractive index $\Delta n(c) = n_{SiON} - n_{sensing}(c)$, where n_{SiON} and $n_{sensing}(c)$ are the

refractive indices of respectively the SiON and sensing material. If $\Delta n(c) = 0$, all optical power will be transferred to the next segment.

If however $\Delta n(c) \neq 0$, then due to the difference in field profiles of both types of segments not all guided mode power launched into one segment will be transferred to the guided mode of the adjacent segment. At the transition radiation will be generated. The amount of power left in the waveguide of course depends on Δn and hence, in the chemo optical sensors we are considering, it is a measure for the concentration of the measurand. If only one transition is used, then the chemically induced change of the loss of guided mode power Δn generally is very small; however, with a sequence of a few thousand transitions, a quite sensitive sensor can be obtained.

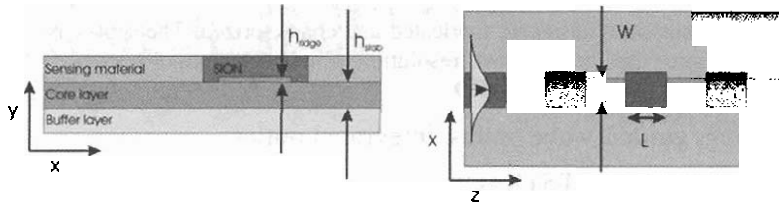


Figure 2. Cross section (left) and top view (right) of an SWS with segmentation in the cladding.

Part of the power radiated out at one transition will be re-captured into the guided mode at one of the next transitions. It is the distance L between two neighboring transitions that determines both the amount and phase of the field that is coupled back into the guided mode. Depending on the phase difference, there can be

constructive or destructive interference between the original guided mode and the radiation coupled back into the guided mode. Although not required, for simplicity reasons we have chosen here for a periodic structure, with an equal length of both segment types. Note however that the principle works for any distribution of segment lengths and that the nature of the distribution itself also is a design parameter. Note also that in the above we silently assumed that no backward propagating modes are generated at the transitions, an assumption which is supported by all our calculations. In the regime of indices used for the sensor backward scattering is negligibly small. We have also verified that higher order Bragg reflections do not influence the operation of the sensor; for the experimental results depicted in figures 5 and 6 the maximum power reflection was calculated to be 0.001

DESIGN

Below we will discuss how the device parameters have been determined, aiming for an optimal sensitivity. The SWS structures have been realized in SiON technology, using a Si wafer as a substrate and Si₃N₄ (index 1.96) as core material. A schematic picture is given in figure 2, whereby the thicknesses of both cladding layers, consisting of SiON (with yet undetermined index) and the sensing material, are chosen to be sufficiently large,

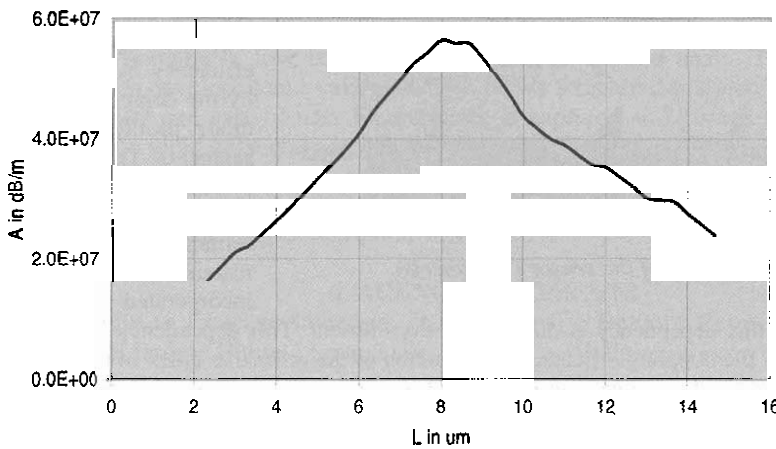


Figure 3 Results of BEP calculations of the parameter A as a function of L .

so that these may be considered to be semi-infinite, for the chosen wavelength, $\lambda=633\text{nm}$, and polarization (TE) and other device parameters. The channel width, which is not a critical quantity for the sensitivity, is put equal to $W=2\mu\text{m}$. The thickness of the core layer, h_{slab} , may, for technological reasons, not be less than 5nm. A small thickness is desirable as then, due to a large lateral contrast between ridge and adjacent sections, the radius of curvature in the applied bends (see below) can be small. So, we have chosen $h_{\text{slab}}=5\text{nm}$. The buffer SiO₂ layer (index 1.45) has a thickness of 2.8 μm , corresponding approximately to an overall thickness (limited by technological considerations) of 5 μm . The buffer layer thickness determines the minimum size of the evanescent modal tail into the substrate, and so the minimum core thickness required to prevent noticeable modal leakage of the TE mode into the substrate. For a core thickness of $h_{\text{core}}=30\text{nm}$, the modal loss is negligible, and as the larger evanescent tail into the sensing

region leads to a larger sensitivity, this value has been chosen. The index of the SiON cladding layer has to be in the range of the sensing material index (see below) and is chosen to be $n_{clad}=1.457$, corresponding to SiO₂. The minimum bend radius has been calculated using C2V software [9], leading to a choice of 300 μ m for the minimum bend radius, corresponding to a negligible bending loss of 10⁻³dB/cm. The designed waveguide channel is multi-modal, but with fiber chip coupling mainly the fundamental mode is excited, and the higher order modes are strongly leaking in the bend sections.

For the calculation of the remaining parameters, being the length of the segments, L , and the total sensor length, L_{sens} , we will use the resolution analysis for SWSs, as given in [6], and which will be repeated here in short. The functional loss of an SWS can be shown to be given in good approximation by

$$\eta(n) = AL_{sens} \Delta n^2, \tag{1}$$

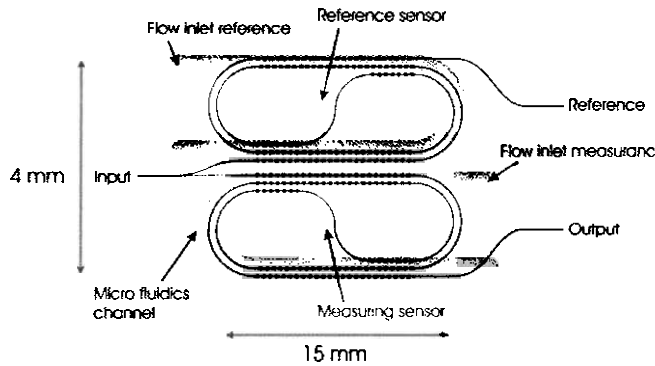


Figure 4. Layout of an SWS with a reference sensor and micro fluidic system.

for small values of the index contrast between the two cladding materials, Δn . Here η is given in dB, n is the index of the sensing material, and A is an important parameter for the quality of the sensor, that has to be optimized. The transmission of the complete device, $T(=P_{out}/P_{in})$ as a function of the sensor length is given by:

$$T(n) = 10^{-0.1(A\Delta n^2 + B)L_{sens}}, \tag{2}$$

where B are the propagation losses due to waveguide imperfections (in dB/m) and where we have neglected the losses due to fiber-chip coupling. The resolution depends on the sensitivity of the sensor which can be written, using equation (2), as follows:

$$S(n) \equiv \partial T / \partial n = -\ln(10)2A\Delta n T(n) / 10. \tag{3}$$

The smallest variation in the transmission that can be detected, δT , is given by the fluctuations in T due to noise in the sensor in, e.g., light source and detector. Then, writing $\delta T=qT$, with q the sum of all relative contributions to the noise, we can write for the index resolution:

$$\delta n = (\partial n / \partial T) \delta T = 5q / [\ln(10)A\Delta n L_{sens}]. \tag{4}$$

From (4) it can be seen that L_{sens} should be as large as possible. On the other hand the output power has to be within the dynamical range of the equipment, defining a minimum transmission T_{min} . Then, with (2) we obtain an optimal value for the sensor length

$$L_{sens,max} = 10 \log T_{min} / (A\Delta n_{max}^2 + B), \tag{5}$$

with Δn_{max} the highest value of Δn that has to be measured. Substituting (5) into (4) the corresponding expression for the index resolution can be obtained:

$$\delta n = q(A\Delta n_{max}^2 + B) / [2 \ln(10) \log(T) \Delta n A]. \tag{6}$$

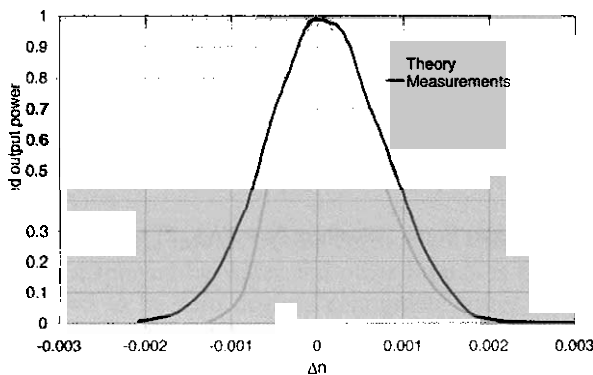


Figure 5. Characteristic spiral SWS, 1/2 rounds.

As might be anticipated, for the best resolution A should be large, and q and B should be small.

The functional losses of the SWS, which are related to the parameter A according to (1) have been calculated as a function of the segment length, L , using the bidirectional eigenmode expansion method (BEP) with C2V software [9], where we have used the effective index method for the reduction of dimensionality from 3D to 2D [10]. The results of the calculation are given in figure 3, from which we find an optimum segment length of $L=8.4\mu$ m. The total length of the sensor depends among

others on the parameter B , as this quantity has to be determined experimentally a large number of sensors, with different sensor lengths, have been fabricated on a single chip.

EXPERIMENTAL RESULTS

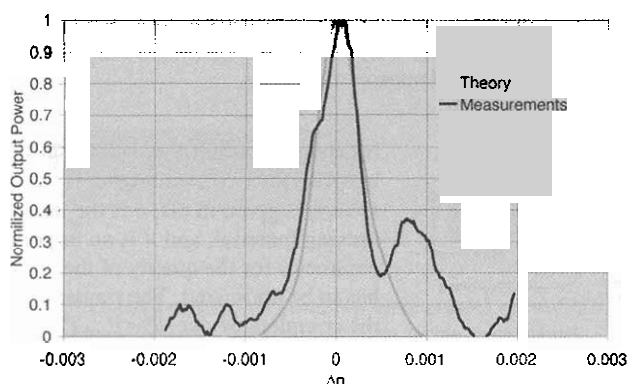


Figure 6. Characteristic spiral SWS, 5½ rounds.

In figure 4 a typical layout of a spiraled SWS is depicted, whereby the reference sensor is added to enable the correction for noise mainly in source intensity and temperature drift. The reference sensor has not been used in the here presented results due to problems with fiber chip coupling. The sensor is supplied with micro-fluidics channels, to enable the application of a variable mixture of ethanol and benzyl alcohol. The corresponding set-up, described in detail in [8], has been built for testing purposes and enables a well controlled index variation of the liquid between 1.36 and 1.54.

Performance characteristics of two SWS spiral sensors with different length are given in figure 5 (for a spiral, containing 1½ rounds and having a total length of the segmented

sections of 3.7 cm) and figure 6 (for a spiral containing 5½ rounds, corresponding with a total length of the segmented sections of 14.1cm). The measurements fit the theory reasonably well.

The index resolution can be estimated from the experimentally and theoretically determined parameters with (6). Assuming $q \sim 0.002$, $B = 2 \text{ dB/cm}$ and $T_{\text{min}} \sim 0.001$, and using the calculated value $A = 6.10^7 \text{ dB/m}$, we arrive at an index resolution of $\delta n = 3.10^{-8}$, for a maximum index variation of $\Delta n_{\text{max}} = 10^{-4}$.

CONCLUSIONS

A novel type of a refractive integrated optical chemical sensor, the spiraled segmented waveguide sensor, has been introduced. This sensor combines a simple technology with a calculated resolution in the refractive index of the chemo-optical transduction layer better than $3 \cdot 10^{-8}$. This sensing principle has been analyzed theoretically and experimentally. Experimental results agree fairly well with theory.

ACKNOWLEDGMENT

This work was supported by the Dutch Technology Foundation STW (grant TOE.5071).

REFERENCES

1. P.V. Lambeck, Integrated Optics for the Chemical Domain, Proc. Of the *ECIO 2001*, pp. 153-163
2. J. Webjorn, F. Laurell, G. Arvidsson, Fabrication of periodically domain-inverted channel waveguides in lithium niobate for second harmonic generation, *J. Lightw. Technol.* 7, pp. 1597-1600, 1989
3. Z. Weissman, I. Hendel, Analysis of periodically segmented waveguide mode expanders, *J. Lightw. Technol.* Vol. 13(10), pp 2053-2081, 1995.
4. Z. Weissman, Evanescent field sensors with periodically segmented waveguides, *Applied-Optics*, Vol. 36(6), pp 1218-1224, 1997.
5. H.J.W.M. Hoekstra, J. van Lith, S. Gaál, P.V. Lambeck, The Spectral Decomposition Method: a Transparent Theory for Losses in Segmented Waveguides, *proceedings ECIO 2003*, pp. 339-342
6. Joris van Lith, Paul.V. Lambeck, Hugo.J.W.M. Hoekstra, Rene. G. Heideman, R.R. Wijn, A segmented waveguide sensor: principle and experiments, *J.Lightw.Technol.* 23, pp. , 2005
7. S. Gaál, doctoral thesis, University of Twente, dec. 2002.
8. J. van Lith, doctoral thesis, University of Twente, 2005.
9. OlympIOs; *C2V software*, version 5.1.12
10. T.Tamir, Topics in Applied Physics volume 7, Springer-Verlag Berlin Heidelberg New York, 2nd edn. 1979.